Multicritical behavior in dissipative Ising models

Vincent R. Overbeck,[1,*] Mohammad F. Maghrebi,[2] Alexey V. Gorshkov,[2] and Hendrik Weimer[1]

[1]*Institut für Theoretische Physik, Leibniz Universität Hannover, Appelstraße 2, 30167 Hannover, Germany*

[2]*Joint Quantum Institute and Joint Center for Quantum Information and Computer Science, NIST/University of Maryland, College Park, Maryland 20742, USA*

We analyze theoretically the many-body dynamics of a dissipative Ising model in a transverse field using a variational approach. We find that the steady-state phase diagram is substantially modified compared to its equilibrium counterpart, including the appearance of a multicritical point belonging to a different universality class. Building on our variational analysis, we establish a field-theoretical treatment corresponding to a dissipative variant of a Ginzburg-Landau theory, which allows us to compute the upper critical dimension of the system. Finally, we present a possible experimental realization of the dissipative Ising model using ultracold Rydberg gases.

I. INTRODUCTION

The continuous transition between a paramagnetic phase and a ferromagnetic phase within the Ising model in a transverse field is one of the most important examples of a quantum phase transition. At finite temperature, thermal fluctuations dominate while the phase transition between the two phases remains continuous [1]. Here, we show that adding dissipation to the model strongly modifies the phase diagram and gives rise to a multicritical point belonging to a different universality class.

Rapid experimental progress in the control of tailored dissipation channels [2–6], combined with prospects to use dissipation for the preparation of interesting many-body states [7–9], has put dissipative quantum many-body systems at the forefront of ultracold atomic physics, quantum optics, and solid-state physics. In particular, systems driven to highly excited Rydberg atoms have emerged as one of the most promising routes [10–28], as the dissipation and interaction properties of Rydberg gases can be very widely tuned [29]. These crucial experimental advances have led to the investigation of driven-dissipative models in a wide range of theoretical works [16,19,22,30–41]. However, the theoretical understanding of dissipative quantum many-body systems is still in its infancy, as many of the concepts and methods from equilibrium many-body systems cannot be applied. As a consequence, little is known even about the most basic dissipative models.

In this paper, we perform a variational analysis of the steady state of dissipative Ising models using a recently introduced variational method. In contrast to the equilibrium case, we find that the continuous transition is replaced by a first-order transition if the dissipation is sufficiently stronger than the transverse field (see Fig. 1). Strikingly, we find that the model gives rise to a multicritical behavior, as the two types of transitions are connected by a tricritical point. This deviation from the equilibrium situation underlines the fact that dissipative many-body systems constitute an independent class of dynamical systems that go beyond the presence of a finite effective

temperature. Furthermore, we establish a field-theoretical treatment of dissipative many-body systems corresponding to a Ginzburg-Landau theory, which allows us to identify the upper critical dimension of the tricritical point. Finally, we give a concrete example of a possible experimental realization of dissipative Ising models based on Rydberg-dressed atoms in optical lattices, showing that the observation of the tricritical point is within reach in present experimental setups.

Spontaneous Z_2-symmetry breaking

Dissipative systems are no longer governed by the unitary Schrödinger equation but have to be described in terms of a quantum master equation instead. Here, we consider the case of a Markovian master equation for the density operator ρ, given in the Lindblad form as

$$\frac{d}{dt}\rho = -i[H,\rho] + \sum_i \left(c_i \rho c_i^\dagger - \frac{1}{2}\{c_i^\dagger c_i, \rho\} \right). \quad (1)$$

Importantly, dissipative quantum systems generically relax towards one or more steady states, which can be found by solving the equation $d\rho/dt = 0$.

For the dissipative Ising model, the Hamiltonian is of the form

$$H = \Delta \sum_i \sigma_z^{(i)} - J \sum_{\langle ij \rangle} \sigma_x^{(i)} \sigma_x^{(j)}, \quad (2)$$

where Δ denotes the strength of the transverse field and J indicates the strength of the ferromagnetic Ising interaction. The quantum jump operators $c_i = \sqrt{\gamma}\sigma_-^{(i)}$ describe dissipative spin flips occurring with a rate γ. Consequently, this dissipative Ising model is a straightforward generalization including Lindblad dynamics. Note that the present model is unrelated to a series of similarly named models, where a strong coupling to the bath is present [42,43] or where explicit time-dependent driving is considered [30]. We would also like to stress that in contrast to previous studies of dissipative Rydberg gases [17,20,22,26,44–46], the present model exhibits a global Z_2 symmetry. Since the dissipation acts in the eigenbasis of the transverse field, the master equation is invariant under applying a σ_z transformation to all the spins. Different driven-dissipative models with Z_2 symmetry have been investigated

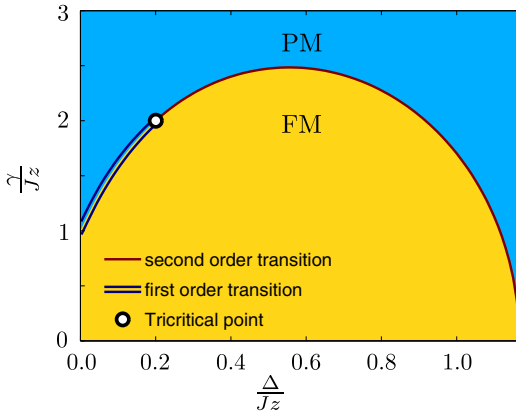---

*vincent.overbeck@itp.uni-hannover.de

FIG. 1. Phase diagram of the three-dimensional dissipative Ising model according to the variational principle based on product states. The system can undergo phase transitions between ferromagnetic (FM) and paramagnetic (PM) phases, which can be either continuous or first order. The continuous and first-order transition lines meet at a tricritical point.

previously [47,48]. Crucially, this Z_2 symmetry can be spontaneously broken by the steady state of the dynamics, constituting a continuous dissipative phase transition. Interestingly, recent results obtained within the Keldysh formalism show that this continuous transition can break down for sufficiently strong dissipation [49], hinting that the dissipative phase diagram is much richer than its equilibrium counterpart.

Here, we will calculate the properties of this steady state using a recently established variational principle [44]. In a spirit similar to equilibrium thermodynamics, where a free-energy functional has to be minimized, we consider a functional for dissipative systems that becomes nonanalytic at a dissipative phase transition. To be specific, we will choose our variational manifold as product states of the form

$$\rho = \prod_i \rho_i, \quad \rho_i = \frac{1}{2}\left(1 + \sum_{\mu \in \{x,y,z\}} \alpha_\mu \sigma_\mu^{(i)}\right). \quad (3)$$

Later on, we will investigate in detail the validity of this approach by explicitly considering fluctuations around product states. In the case of product states, the variational principle is based on the minimization of $D = \sum_{\langle ij \rangle} ||\dot{\rho}_{ij}||$ [44]. Here, the norm $||\dot{\rho}_{ij}||$ is given by the trace norm, $||x|| = \text{Tr}\{|x|\}$, and $\dot{\rho}_{ij}$ is the reduced two-site operator obtained after taking the partial trace of the time derivative $d\rho/dt$, according to $\dot{\rho}_{ij} = \text{Tr}_{i/j}\{d\rho/dt\}$. As our model is translationally invariant, it is sufficient to consider the variational norm of a single bond $||\dot{\rho}_{ij}||$. Then, the steady state is approximated by the variational minimization procedure $||\dot{\rho}_{ij}|| \to$ min. We would like to stress that although our ansatz according to Eq. (3) is a product state, the variational principle differs from a pure mean-field decoupling as $\dot{\rho}_{ij}$ includes the time derivative of correlation functions [44].

Next, we perform an expansion of the variational norm $||\dot{\rho}_{ij}||$ in the order parameter $\phi \equiv \langle \sigma_x \rangle$, in close analogy to Landau theory for equilibrium phase transitions. The degree of nonanalyticity of the order parameter can be used to classify the phase transition: a discontinuous jump indicates a

first-order transition, while a diverging derivative corresponds to a second-order transition. Within our product-state approach, we choose the variational parameters according to

$$\alpha = (\langle \sigma_x \rangle, \langle \sigma_y \rangle, \langle \sigma_z \rangle) = (\phi, c\phi, \lambda). \quad (4)$$

Separating the order parameter ϕ in the $\langle \sigma_y \rangle$ expression has the advantage that c becomes an analytic function. In the following, we will choose λ such that we always have a pure state satisfying $|\alpha|^2 = 1$. Taking λ as an independent variational parameter does not lead to a significant difference in our results; that is, solutions close to phase boundaries exhibit high purity.

Expanding $||\dot{\rho}_{ij}||$ up to the sixth order in ϕ leads to

$$||\dot{\rho}_{ij}|| = u_0 + u_2\phi^2 + u_4\phi^4 + u_6\phi^6 \quad (5)$$

as odd powers in ϕ vanish because of the Z_2 symmetry. From the exact diagonalization of the 4×4 matrix $\dot{\rho}_{ij}$, we can readily calculate the expansion coefficients u_n as functions of the coupling constants J, Δ, and γ, as well as the coordination number z and the variational parameter c.

As the next step, we determine the variational solution for the parameter c. According to our ansatz of Eq. (4), the nonanalytic behavior is contained in ϕ, whereas c is a smooth function. Therefore, the value of c close to phase boundaries is fixed by its behavior far away from phase transitions. In the latter regime, ϕ^2 is the leading order of the variational functional (A1), which allows us to find the variational minimum by minimizing only u_2. Doing so with respect to c leads to

$$c = \frac{J\gamma z}{(\gamma/2)^2 + 4\Delta^2}. \quad (6)$$

Using that expression for c, there is only the order parameter ϕ left as an independent variational parameter. Consequently, we have successfully constructed the equivalent of Landau theory for dissipative phase transitions and determined all expansion parameters from the microscopic quantum master equation [50].

The dissipative functional of Eq. (A1) is mathematically equivalent to the free-energy functional of a ϕ^6 theory, whose possible phases are known [51]. For $u_4 > 0$, the ϕ^6 term is irrelevant, and there is a continuous Ising transition between a paramagnetic phase ($u_2 > 0$) and a ferromagnetic phase ($u_2 < 0$). Close to the transition, the order parameter behaves as $\phi = \pm(|u_2|/2u_4)^{1/2}$. In the equilibrium Ising model, u_4 is always positive, but here, we find that this is not the case when adding dissipation. If the dissipation rate γ is sufficiently larger than the transverse field Δ, u_4 will become negative, which substantially alters the phase diagram of the model. In order to find a stable variational solution, it is then necessary to also consider the ϕ^6 term of the series expansion. We find that the variational norm has three different minima, which transforms the transition between the paramagnetic and the ferromagnetic phase into a first-order transition (see Fig. 2). Remarkably, the ϕ^6 theory exhibits a tricritical point at $u_2 = u_4 = 0$, which belongs to a universality class different from that of the Ising transition. This change of the universality class can be seen from the scaling of the order parameter along the $u_4 = 0$ line, $\phi = \pm(|u_2|/3u_6)^{1/4}$, which exhibits a different critical
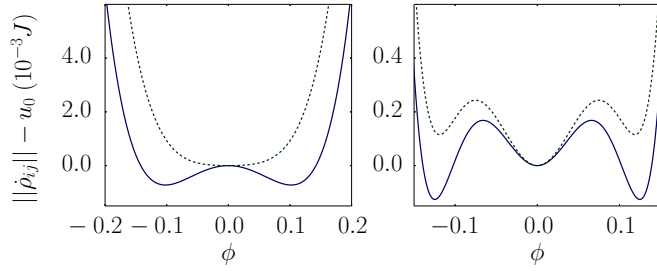
FIG. 2. Expansion in the variational norm $||\dot{\rho}_{ij}||$ to the sixth order in ϕ close to the second-order transition (left) and close to the first-order transition (right). In the ferromagnetic phase, the minimal variational norm is found at $\phi \neq 0$ (solid lines). In the paramagnetic phase, the global minimum is located at $\phi = 0$ (dashed lines).

exponent [52]. We have also confirmed the validity of our series expansion in ϕ by comparison to a numerical minimization of the variational norm including all orders. The full phase diagram of the dissipative Ising model is shown in Fig. 1.

II. FLUCTUATIONS

So far, we have neglected the fact that the true steady state of the system is not a product state. In reality, there will be fluctuations in the system that lead to deviations from the variational solution of the series expansion of Eq. (A1). Importantly, the strength of these fluctuations is inherently determined by the value of the variational norm at the variational minimum. In close analogy to equilibrium transitions, we can analyze at which point fluctuations lead to a breakdown of the product-state ansatz. To take these fluctuations into account, it is first necessary to introduce spatial inhomogeneities of the order parameter. Then, fluctuations generate such spatial inhomogeneities in the same manner as in equilibrium systems. To this end, we will take long-wavelength inhomogeneities into account by performing a gradient expansion of the variational norm. Then we can evaluate the equivalent of the Ginzburg criterion [53] to determine the range of validity of our effective theory.

We first allow for spatial variations within our product-state ansatz. Then the variational functional can be written as [54]

$$
D = \sum_{\langle ij \rangle} ||\dot{\rho}_{ij}|| = \sum_{\langle ij \rangle} z \left[\frac{J}{2} \left(1 - \frac{1}{z} \right) + \frac{J'}{z} \right] (\phi_i - \phi_j)^2 \\
+ \sum_i z \left[u_0 + u_2 \phi_i^2 + u_4 \phi_i^4 + u_6 \phi_i^6 \right], \quad (7)
$$

where $\phi_i = \langle \sigma_x^{(i)} \rangle$ is the value of the order parameter field at site i and the coupling constant J' is given by

$$
J' = -\frac{J}{4} + \frac{\left(\frac{\gamma}{4} \right)^2 + \Delta^2}{4J} + \frac{J\gamma^2}{\gamma^2 + 16\Delta^2}. \quad (8)
$$

The first term in Eq. (7) describes spatial variations of the order parameter to lowest order, while the other terms correspond to the original series expansion of Eq. (A1). For a finite value of ϕ_i, the eigenbasis of ρ_i is rotated away from the eigenbasis of σ_z. Consequently, the coupling constant J' also depends on γ and Δ. Taking the continuum limit, we arrive at a

Ginzburg-Landau-like functional for the variational norm,

$$
D[\Phi] = z \int d^d x u_0 + v_2 (\nabla \Phi)^2 + u_2 \Phi^2 + u_4 \Phi^4 + u_6 \Phi^6, \quad (9)
$$

where the order parameter ϕ follows from spatial averaging of the fluctuating field $\Phi(x)$. The gradient term v_2 can then be readily identified as

$$
v_2 = \left[\frac{J'}{z} + \frac{J}{2} \left(1 - \frac{1}{z} \right) \right] a^2, \quad (10)
$$

where a is the lattice spacing, which we set to unity in the following.

Following from the existence of a dynamical symmetry [31], fluctuations in the system will exhibit thermal statistics at long wavelengths [49]. Hence, we can characterize the strength of these fluctuations by an effective temperature T_{eff}. Crucially, the strength of fluctuations is determined by the value of the variational norm, as its value is a measure of how much the exact steady state deviates from the product-state solution. However, we have to renormalize the variational norm to get an intensive quantity. Then we find that the effective temperature is connected to the variational norm according to $T_{\text{eff}} = \frac{z}{2} ||\dot{\rho}_{ij}||$, where the variational norm $||\dot{\rho}_{ij}||$ is to be evaluated in the absence of spatial inhomogeneities; that is, the choice of i and j does not matter. In the paramagnetic phase, the variational solution results, according to the minimization of Eq. (A1), in $\alpha = (0, 0, -1)$, which corresponds to a variational norm of $||\dot{\rho}_{ij}|| = 2J$. Remarkably, the resulting effective temperature on the Ising transition line is given by $T_{\text{eff}} = zJ$, which matches exactly the result found within the Keldysh formalism [49].

Using this effective temperature, we can now evaluate the strength of fluctuations around the homogeneous solution. Considering Gaussian fluctuations, we find for the mean-square fluctuations

$$
\langle [\phi - \Phi]^2 \rangle = \frac{T_{\text{eff}}}{2v_2} \xi^{2-d} w^d, \quad (11)
$$

where $\xi^2 = v_2 / 2|u_2|$ is the square of the correlation length, d is the number of spatial dimensions, and $w = 0.0952$ is a numerical constant [53]. Following the approach of the Ginzburg criterion, we compare these mean squared fluctuations to the square of the order parameter close to the multicritical point, which results in

$$
\frac{\langle [\phi - \Phi]^2 \rangle}{\phi^2} = \frac{\sqrt{3}}{4} w^d v_2^{-d/2} u_0 \sqrt{u_6} u_2^{(d-3)/2}. \quad (12)
$$

The self-consistency of our effective theory is determined by the exponent of the u_2 term. For $d > 3$, the exponent is positive, and the relative strength of fluctuations is decreasing if $(\Delta/zJ, \gamma/zJ) \to (\Delta/Jz, \gamma/zJ)_{TC}$, where $(\Delta/Jz, \gamma/zJ)_{TC}$ is the value of Δ and γ at the multicritical point; that is, our effective theory becomes self-consistent. For $d < 3$, the exponent is negative, and fluctuations diverge close to the multicritical point. Hence, $d = 3$ is the upper critical dimension of the multicritical point, above which critical exponents derived within Landau theory according to Eq. (A1) become exact. At the experimentally accessible case of $d = 3$,
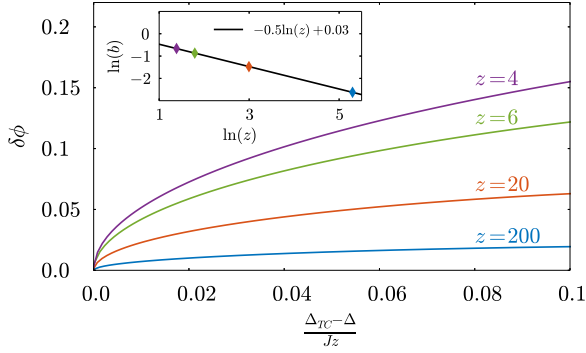
FIG. 3. First-order jump $\delta\phi$ versus $\frac{\Delta_{TC}-\Delta}{Jz}$ along the first-order line for $z = 4, 6, 20$, and 200. Inset: Logarithm of b, which is obtained from the fit of $\delta\phi$ according to Eq. (13), versus $\ln(z)$ and the corresponding fit (solid line).
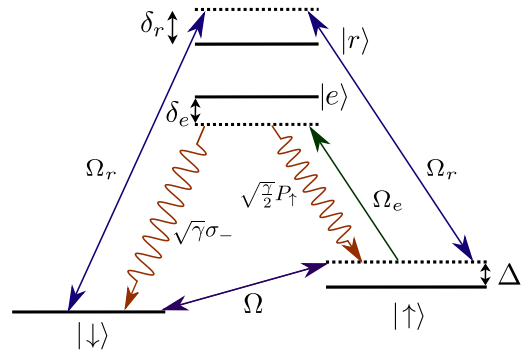

FIG. 4. Four-level scheme with the ground states corresponding to the two spin configurations $|\uparrow\rangle$ and $|\downarrow\rangle$ and the dressed Rydberg state $|r\rangle$. The dissipation is realized via the $|e\rangle$ state.

one can expect merely logarithmic corrections to the Landau theory exponents [55]. We would like to point out that the same result can also be obtained from a renormalization-group calculation, which also allows us to evaluate corrections to the position of the tricritical point in a systematic way. While the position of the tricritical point is shifted significantly on including the renormalization-group corrections in three dimensions, we find that the strength of the shift decreases exponentially with increasing spatial dimensions [56].

III. COMPARISON TO MEAN-FIELD RESULTS

In contrast to the equilibrium case, the mean field does not describe the correct physics at the upper critical dimension in our open system as it misses the first-order transition and the tricritical point [49]. Still, mean-field theory becomes exact as $d \to \infty$, where the variational approach and mean-field theory agree. We now investigate in detail how the variational solution behaves as the dimensionality is increased. Specifically, we consider the value of the jump of the order parameter at the first-order transition $\delta\phi$, which is given by

$$\delta\phi = b\left(\frac{\Delta_{TC} - \Delta}{Jz}\right)^{1/2}, \quad (13)$$

where Δ_{TC} is the value of Δ at the tricritical point. Remarkably, the tricritical point remains at a finite value of Δ even when the dimensionality of the system diverges, asymptotically approaching $(\Delta/zJ, \gamma/zJ)_{TC} = (0.22, 1.66)$ in the limit of infinite spatial dimensions. Consequently, the mean-field result is not recovered in a way that leads to a disappearance of the tricritical point. Instead, the prefactor b decreases according to $b \sim 1/\sqrt{d}$ as the dimensionality of the system is increased (see Fig. 3). Hence, for any finite dimension, the tricritical point can be observed, and the mean-field prediction is incorrect. Therefore, our results present further evidence (see also [45,49]) that, for dissipative systems, mean-field theory can be qualitatively incorrect even above the upper critical dimension. Instead, it appears that only the variational principle is capable of correctly describing this regime of high dimensionality. Finally, we find that, according to our variational analysis, the location of the first-order transition at the $\Delta = 0$ line approaches the value $\gamma = 0$ with

increasing dimension. This behavior is consistent with analytic arguments showing that there is no ferromagnetic phase at $\Delta = 0$ in any dimension [57].

IV. EXPERIMENTAL REALIZATION

For an experimental implementation of the dissipative Ising model, we turn to a scenario where a Rydberg state is weakly admixed to the electronic ground-state manifold [58–62]. Such Rydberg dressing of ground state atoms has recently been observed in several experiments [63–65]. Here, we consider the dressing performed within a Raman scheme, where two ground states are coupled to the same Rydberg state (see Fig. 4). We obtain the effective Hamiltonian for the dressed system based on fourth-order degenerate perturbation theory [66,67] in Ω_r/δ_r, which generically has the form

$$H = \Delta \sum_i \sigma_z^{(i)} + \Omega' \sum_i \sigma_x^{(i)} - \sum_{ij} J_{ij} \sigma_x^{(i)} \sigma_x^{(j)} + \text{const.}$$

$$(14)$$

This Hamiltonian is not yet in a Z_2-symmetric form as the Ω' term breaks the symmetry. Crucially, this symmetry-breaking term can be canceled by including a direct coupling Ω between the two ground states into our perturbative analysis (see Fig. 4). Choosing $\Omega_r = \delta_r/10$ and $\Delta \sim |J_{\langle ij\rangle}| \sim \Omega_r^4/\delta_r^3$ allows one to suppress the strength of all Z_2 symmetry-breaking terms by several orders of magnitude. Tuning the Rydberg interaction strength V such that $V = 3\delta_r$ ensures that the effective interaction potential can be cut off beyond nearest neighbors.

Finally, we realize the dissipative terms by performing optical pumping from the spin-up into the spin-down state. In the case of ^{87}Rb, this can be realized by choosing $|\uparrow\rangle = |5S_{1/2}, F = 2, m_F = 2\rangle$, $|\downarrow\rangle = |5S_{1/2}, F = 2, m_F = 1\rangle$, and $|e\rangle = |5P_{3/2}, F = 3, m_F = 2\rangle$. Note that this will result in an additional dephasing term described by the jump operator $P_\uparrow = |\uparrow\rangle\langle\uparrow|$; however, this term preserves the Z_2 symmetry and is also weaker than the dissipative spin flip [68]. Finally, we would like to mention that the dissipative Ising model can also be realized within the experimental implementation suggested in [47], at the expense of requiring additional laser fields.

APPENDIX A: EXPANSION COEFFICIENTS OF THE VARIATIONAL NORM

The expansion coefficients of the variational norm according to

$$||\dot{\rho}_{ij}|| = u_0 + u_2\phi^2 + u_4\phi^4 + u_6\phi^6 \tag{A1}$$

are given by

$$u_0 = 2J, \ u_2 = \frac{\frac{\gamma^2}{16} + \Delta^2}{J} + J\left(\frac{16\Delta^2 z^2}{\gamma^2 + 16\Delta^2} - 1\right) - 2\Delta z, \tag{A2}$$

$$
\begin{aligned}
u_4 = -\frac{1}{512J^3(\gamma^2 + 16\Delta^2)^4}\{&(\gamma^2 + 16\Delta^2)^6 + 8192\gamma^5 J^7 z^4 + 131072\gamma^4\Delta^2 J^6 z^4 - 1024\gamma^2 J^5 z^2(\gamma^2 + 16\Delta^2)^2(8\Delta z - \gamma)\\
&+ 16384\Delta^2 J^4 z^2(\gamma^2 + 16\Delta^2)^2(\gamma^2 + 4\Delta^2 z^2) + 32J^3(\gamma^2 + 16\Delta^2)^3[\gamma^3 + 16\gamma\Delta^2 + 256\Delta^3 z(1 - 2z^2) + 16\gamma^2\Delta z]\\
&- 64J^2(\gamma^2 + 16\Delta^2)^4[\gamma^2 + 8\Delta^2(1 - 3z^2)] - 64\Delta J z(\gamma^2 + 16\Delta^2)^5\},
\end{aligned}
\tag{A3}
$$

$$
\begin{aligned}
u_6 = -\frac{1}{24576J^5(\gamma^2 + 16\Delta^2)^6}\{&-(\gamma^2 + 16\Delta^2)^9 + 1048576\gamma^7 J^{11} z^6 - 524288\gamma^6 J^{10} z^6(\gamma^2 - 16\Delta^2)\\
&- 65536\gamma^4 J^9 z^4(\gamma^2 + 16\Delta^2)[-3\gamma^3 + 16\gamma\Delta^2(2z^2 - 3) + 8\gamma^2\Delta z + 128\Delta^3 z]\\
&- 131072\gamma^4 J^8 z^4(\gamma^2 + 16\Delta^2)[\gamma^4 - 8\gamma^2\Delta^2 + 128\Delta^4(2z^2 - 3) - 2\gamma^3\Delta z - 32\gamma\Delta^3 z]\\
&+ 4096\gamma^2 J^7 z^2(\gamma^2 + 16\Delta^2)^2[\gamma^5(3 - 2z^2) - 96\gamma^3\Delta^2(z^2 - 1) + 1536\gamma^2\Delta^3 z(z^2 - 1)\\
&+ 256\gamma\Delta^4(3 - 4z^2) + 4096\Delta^5 z(2z^2 - 3) - 48\gamma^4\Delta z] - 2048J^6 z^2(\gamma^2 + 16\Delta^2)^3[5\gamma^6 + 64\gamma^4\Delta^2(3z^2 - 1)\\
&+ 256\gamma^2\Delta^4(14z^2 - 9) + 8192\Delta^6 z^2(z^2 - 1) - 16\gamma^5\Delta z - 256\gamma^3\Delta^3 z] - 256J^5(\gamma^2 + 16\Delta^2)^4[\gamma^5(4z^2 - 1)\\
&- 8\gamma^4\Delta z(4z^2 + 3) + 32\gamma^3\Delta^2(3z^2 - 1) - 256\gamma^2\Delta^3 z(4z^2 + 3) + 256\gamma\Delta^4(2z^2 - 1) - 6144\Delta^5 z(1 - 2z^2)^2]\\
&- 256J^4(\gamma^2 + 16\Delta^2)^5[5\gamma^4 + 16\gamma^2\Delta^2(7 - 10z^2) + 256\Delta^4(15z^4 - 12z^2 + 2) - 4\gamma^3\Delta z - 64\gamma\Delta^3 z]\\
&- 32J^3(\gamma^2 + 16\Delta^2)^6[\gamma^3 + 16\gamma\Delta^2 + 1280\Delta^3 z(1 - 2z^2) + 112\gamma^2\Delta z]\\
&+ 16J^2(\gamma^2 + 16\Delta^2)^7[5\gamma^2 + 48\Delta^2(1 - 5z^2)] + 96\Delta J z(\gamma^2 + 16\Delta^2)^8\}.
\end{aligned}
\tag{A4}
$$

APPENDIX B: DERIVATION OF THE VARIATIONAL NORM INCLUDING SPATIAL FLUCTUATIONS

In this appendix, we derive Eq. (9) in the main text. In order to evaluate the consistency of our product-state ansatz, we allow spatial inhomogeneities of the order parameter field. Consequently, the variational parameter $\phi_i = \langle \sigma_x^{(i)} \rangle$ has a different value at each site i in our ansatz for the product-state density matrix ρ.

Expanding the variational norm $||\dot{\rho}_{ij}||$ with respect to the order parameter, we get terms of the form $u_{2n}\phi_i^{2n}$, which correspond to the terms of the expansion in the homogeneous case. Due to the fluctuations of the order parameter field, we get additional gradient terms of the form $v_2(\phi_k - \phi_l)^2$ in the lowest (quadratic) order, where k and l are neighboring sites. Here, we have a contribution to the variational norm $||\dot{\rho}_{ij}||$ from the difference between sites i and j and from the gradient between sites i and j and their nearest surrounding sites k and l, respectively.

The variational functional can then be written as

$$
\begin{aligned}
D = \sum_{\langle ij\rangle} ||\dot{\rho}_{ij}|| = \sum_{\langle ijkl\rangle} &\frac{J}{2}(z - 1)(\phi_i - \phi_k)^2\\
&+ \frac{J}{2}(z - 1)(\phi_j - \phi_l)^2 + J'(\phi_i - \phi_j)^2\\
&+ \sum_{\langle ij\rangle}[u_0 + u_2\phi_i^2 + u_4\phi_i^4 + u_6\phi_i^6],
\end{aligned}
\tag{B1}
$$

with

$$J' = -\frac{J}{4} + \frac{\left(\frac{\gamma}{4}\right)^2 + \Delta^2}{4J} + \frac{J\gamma^2}{\gamma^2 + 16\Delta^2}. \tag{B2}$$

In the long-wavelength limit, we have $\phi_i - \phi_k = \phi_j - \phi_l = \phi_i - \phi_j$, and after factoring out the coordination number z we

arrive at

$$D = \sum_{\langle ij \rangle} z \left[\frac{J}{2}\left(1 - \frac{1}{z}\right) + \frac{J'}{z} \right](\phi_i - \phi_j)^2 \qquad (B3)$$

$$+ \sum_i z\left[u_0 + u_2\phi_i^2 + u_4\phi_i^4 + u_6\phi_i^6\right].$$

APPENDIX C: RENORMALIZATION-GROUP CORRECTION OF THE TRICRITICAL POINT

In the following, we will calculate the shift of the tricritical point when renormalization-group corrections of the u_4 term are included. Starting with the Ginzburg-Landau functional

$$D[\Phi] = z \int d^d x\, u_0 + v_2(\nabla\Phi)^2 + u_2\Phi^2 + u_4\Phi^4 + u_6\Phi^6,$$
$$(C1)$$

a perturbative momentum-space renormalization-group analysis leads to the linear flow equations [69]

$$\frac{du_2}{dl} = 2u_2 + c_1u_4 + c_2u_6, \qquad (C2)$$

$$\frac{du_4}{dl} = (4-d)u_4 + c_3u_6, \qquad (C3)$$

$$\frac{du_6}{dl} = (3-d)u_6. \qquad (C4)$$

Here, c_i are constants that follow from the one-loop expansion of the interaction terms. In particular, the c_3u_6 term stems from the one-loop diagram shown in Fig. 5. The value of the c_3 coefficient is given by

$$c_3 = \frac{2^{-d}15S_d}{\pi^2 v_2}, \qquad (C5)$$

where S_d is the surface area of the d-dimensional unit sphere. Here, we made a cutoff of the momentum-space integral at $\Lambda = \pi/a$, where $a = 1$ is the lattice spacing.
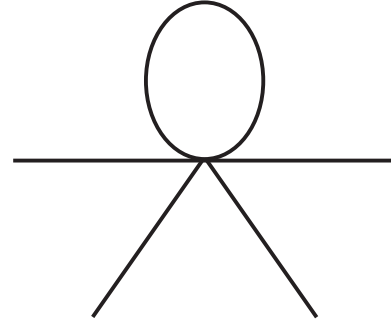

FIG. 5. Diagrammatic visualization of the one-loop correction of the u_4 term. The branches represent the order parameter field in fourth order; the circle stands for the contracted part of the momentum space integral.

In the following, we choose $u_2(0)$ such that we arrive at the fixed point u_2^* corresponding to the Ising critical line. Then, the solution to the second equation will tell us about the nature of the transition [70]. For $u_4^* = \infty$, we have the conventional Ising transition, as the renormalized u_4 is positive. For $u_4^* = -\infty$, we get the first-order transition, while $u_4^* = 0$ is the tricritical point (in $d \geqslant 3$). Depending on the initial values $u_4(0)$ and $u_6(0)$, we may end up in any of these fixed points, allowing us to relate the microscopic coupling constants $u_4(0)$ and $u_6(0)$ to the nature of the transition and hence to the position of the tricritical point. Using $\epsilon = 3 - d$, we arrive at the solutions

$$u_4(l) = u_4(0)e^{(\epsilon+1)l} + c_3u_6(0)[e^{(\epsilon+1)l} - e^{\epsilon l}], \qquad (C6)$$

$$u_6(l) = u_6(0)e^{\epsilon l}, \qquad (C7)$$

with $\epsilon = 3 - d$. From the first equation, we can immediately see that the sign of the fixed point depends on the sign of $u_4(0) + c_3u_6(0)$. Hence, the position of the tricritical point is shifted from $u_4 = 0$ in Landau theory to $u_4 = -c_3u_6$ by the one-loop correction. For $d = 3$, we find that the shifted tricritical point is located at $(\Delta/Jz, \gamma/Jz)_{\text{TC}} = (0.023, 0.35)$. In higher dimensions, the deviation from the variational solution of the tricritical point decreases exponentially with the number of spatial dimensions.

[1] S. Sachdev, *Quantum Phase Transitions* (Cambridge University Press, Cambridge, 1999).

[2] N. Syassen, D. M. Bauer, M. Lettner, T. Volz, D. Dietze, J. J. García-Ripoll, J. I. Cirac, G. Rempe, and S. Dürr, Strong dissipation inhibits losses and induces correlations in cold molecular gases, Science **320**, 1329 (2008).

[3] K. Baumann, C. Guerlin, F. Brennecke, and T. Esslinger, Dicke quantum phase transition with a superfluid gas in an optical cavity, Nature (London) **464**, 1301 (2010).

[4] J. T. Barreiro, M. Müller, P. Schindler, D. Nigg, T. Monz, M. Chwalla, M. Hennrich, C. F. Roos, P. Zoller, and R. Blatt, An open-system quantum simulator with trapped ions, Nature (London) **470**, 486 (2011).

[5] H. Krauter, C. A. Muschik, K. Jensen, W. Wasilewski, J. M. Petersen, J. I. Cirac, and E. S. Polzik, Entanglement Generated by

Dissipation and Steady State Entanglement of Two Macroscopic Objects, Phys. Rev. Lett. **107**, 080503 (2011).

[6] G. Barontini, R. Labouvie, F. Stubenrauch, A. Vogler, V. Guarrera, and H. Ott, Controlling the Dynamics of an Open Many-Body Quantum System with Localized Dissipation, Phys. Rev. Lett. **110**, 035302 (2013).

[7] S. Diehl, A. Micheli, A. Kantian, B. Kraus, H. P. Büchler, and P. Zoller, Quantum states and phases in driven open quantum systems with cold atoms, Nat. Phys. **4**, 878 (2008).

[8] F. Verstraete, M. M. Wolf, and J. I. Cirac, Quantum computation and quantum-state engineering driven by dissipation, Nat. Phys. **5**, 633 (2009).

[9] H. Weimer, M. Müller, I. Lesanovsky, P. Zoller, and H. P. Büchler, A Rydberg quantum simulator, Nat. Phys. **6**, 382 (2010).

[10] U. Raitzsch, R. Heidemann, H. Weimer, B. Butscher, P. Kollmann, R. Löw, H. P. Büchler, and T. Pfau, Investigation of dephasing rates in an interacting Rydberg gas, New J. Phys. **11**, 055014 (2009).

[11] C. Carr, R. Ritter, C. G. Wade, C. S. Adams, and K. J. Weatherill, Nonequilibrium Phase Transition in a Dilute Rydberg Ensemble, Phys. Rev. Lett. **111**, 113901 (2013).

[12] N. Malossi, M. M. Valado, S. Scotto, P. Huillery, P. Pillet, D. Ciampini, E. Arimondo, and O. Morsch, Full Counting Statistics and Phase Diagram of a Dissipative Rydberg Gas, Phys. Rev. Lett. **113**, 023006 (2014).

[13] H. Schempp, G. Günter, M. Robert-de Saint-Vincent, C. S. Hofmann, D. Breyel, A. Komnik, D. W. Schönleber, M. Gärttner, J. Evers, S. Whitlock, and M. Weidemüller, Full Counting Statistics of Laser Excited Rydberg Aggregates in a One-Dimensional Geometry, Phys. Rev. Lett. **112**, 013002 (2014).

[14] A. Urvoy, F. Ripka, I. Lesanovsky, D. Booth, J. P. Shaffer, T. Pfau, and R. Löw, Strongly Correlated Growth of Rydberg Aggregates in a Vapor Cell, Phys. Rev. Lett. **114**, 203002 (2015).

[15] T. M. Weber, M. Honing, T. Niederprum, T. Manthey, O. Thomas, V. Guarrera, M. Fleischhauer, G. Barontini, and H. Ott, Mesoscopic Rydberg-blockaded ensembles in the superatom regime and beyond, Nat. Phys. **11**, 157 (2015).

[16] E. A. Goldschmidt, T. Boulier, R. C. Brown, S. B. Koller, J. T. Young, A. V. Gorshkov, S. L. Rolston, and J. V. Porto, Anomalous Broadening in Driven Dissipative Rydberg Systems, Phys. Rev. Lett. **116**, 113001 (2016).

[17] T. E. Lee, H. Häffner, and M. C. Cross, Antiferromagnetic phase transition in a nonequilibrium lattice of Rydberg atoms, Phys. Rev. A **84**, 031402 (2011).

[18] J. Honer, R. Löw, H. Weimer, T. Pfau, and H. P. Büchler, Artificial Atoms Can Do More Than Atoms: Deterministic Single Photon Subtraction from Arbitrary Light Fields, Phys. Rev. Lett. **107**, 093601 (2011).

[19] A. W. Glaetzle, R. Nath, B. Zhao, G. Pupillo, and P. Zoller, Driven-dissipative dynamics of a strongly interacting Rydberg gas, Phys. Rev. A **86**, 043403 (2012).

[20] C. Ates, B. Olmos, J. P. Garrahan, and I. Lesanovsky, Dynamical phases and intermittency of the dissipative quantum Ising model, Phys. Rev. A **85**, 043620 (2012).

[21] M. Lemeshko and H. Weimer, Dissipative binding of atoms by non-conservative forces, Nat. Commun. **4**, 2230 (2013).

[22] A. Hu, T. E. Lee, and C. W. Clark, Spatial correlations of one-dimensional driven-dissipative systems of Rydberg atoms, Phys. Rev. A **88**, 053627 (2013).

[23] M. Höning, D. Muth, D. Petrosyan, and M. Fleischhauer, Steady-state crystallization of Rydberg excitations in an optically driven lattice gas, Phys. Rev. A **87**, 023401 (2013).

[24] J. Otterbach and M. Lemeshko, Dissipative Preparation of Spatial Order in Rydberg-Dressed Bose-Einstein Condensates, Phys. Rev. Lett. **113**, 070401 (2014).

[25] J. Sanders, R. van Bijnen, E. Vredenbregt, and S. Kokkelmans, Wireless Network Control of Interacting Rydberg Atoms, Phys. Rev. Lett. **112**, 163001 (2014).

[26] M. Hoening, W. Abdussalam, M. Fleischhauer, and T. Pohl, Antiferromagnetic long-range order in dissipative Rydberg lattices, Phys. Rev. A **90**, 021603 (2014).

[27] M. Marcuzzi, E. Levi, S. Diehl, J. P. Garrahan, and I. Lesanovsky, Universal Nonequilibrium Properties of Dissipative Rydberg Gases, Phys. Rev. Lett. **113**, 210401 (2014).

[28] M. Marcuzzi, M. Buchhold, S. Diehl, and I. Lesanovsky, Absorbing State Phase Transition with Competing Quantum and Classical Fluctuations, Phys. Rev. Lett. **116**, 245701 (2016).

[29] R. Löw, H. Weimer, J. Nipper, J. B. Balewski, B. Butscher, H. P. Büchler, and T. Pfau, An experimental and theoretical guide to strongly interacting Rydberg gases, J. Phys. B **45**, 113001 (2012).

[30] G. Goldstein, C. Aron, and C. Chamon, Driven-dissipative Ising model: Mean-field solution, Phys. Rev. B **92**, 174418 (2015).

[31] L. M. Sieberer, S. D. Huber, E. Altman, and S. Diehl, Dynamical Critical Phenomena in Driven-Dissipative Systems, Phys. Rev. Lett. **110**, 195301 (2013).

[32] R. M. Wilson, K. W. Mahmud, A. Hu, A. V. Gorshkov, M. Hafezi, and M. Foss-Feig, Collective phases of strongly interacting cavity photons, Phys. Rev. A **94**, 033801 (2016).

[33] A. Le Boité, G. Orso, and C. Ciuti, Steady-State Phases and Tunneling-Induced Instabilities in the Driven Dissipative Bose-Hubbard Model, Phys. Rev. Lett. **110**, 233601 (2013).

[34] C. Joshi, F. Nissen, and J. Keeling, Quantum correlations in the one-dimensional driven dissipative XY model, Phys. Rev. A **88**, 063835 (2013).

[35] A. Tomadin, V. Giovannetti, R. Fazio, D. Gerace, I. Carusotto, H. E. Türeci, and A. Imamoglu, Signatures of the superfluid-insulator phase transition in laser-driven dissipative nonlinear cavity arrays, Phys. Rev. A **81**, 061801 (2010).

[36] A. Tomadin, S. Diehl, and P. Zoller, Nonequilibrium phase diagram of a driven and dissipative many-body system, Phys. Rev. A **83**, 013611 (2011).

[37] J. Jin, D. Rossini, M. Leib, M. J. Hartmann, and R. Fazio, Steady-state phase diagram of a driven QED-cavity array with cross-Kerr nonlinearities, Phys. Rev. A **90**, 023827 (2014).

[38] J. Marino and S. Diehl, Driven Markovian Quantum Criticality, Phys. Rev. Lett. **116**, 070407 (2016).

[39] E. G. Dalla Torre, E. Demler, T. Giamarchi, and E. Altman, Quantum critical states and phase transitions in the presence of non-equilibrium noise, Nat. Phys. **6**, 806 (2010).

[40] E. Mascarenhas, H. Flayac, and V. Savona, Matrix-product-operator approach to the nonequilibrium steady state of driven-dissipative quantum arrays, Phys. Rev. A **92**, 022116 (2015).

[41] J. Cui, J. I. Cirac, and M. C. Bañuls, Variational Matrix Product Operators for the Steady State of Dissipative Quantum Systems, Phys. Rev. Lett. **114**, 220601 (2015).

[42] P. Werner, K. Völker, M. Troyer, and S. Chakravarty, Phase Diagram and Critical Exponents of a Dissipative Ising Spin Chain in a Transverse Magnetic Field, Phys. Rev. Lett. **94**, 047201 (2005).

[43] P. Werner, M. Troyer, and S. Sachdev, Quantum spin chains with site dissipation, J. Phys. Soc. Jpn. **74**, 67 (2005).

[44] H. Weimer, Variational Principle for Steady States of Dissipative Quantum Many-Body Systems, Phys. Rev. Lett. **114**, 040402 (2015).

[45] H. Weimer, Variational analysis of driven-dissipative Rydberg gases, Phys. Rev. A **91**, 063401 (2015).

[46] V. R. Overbeck and H. Weimer, Time evolution of open quantum many-body systems, Phys. Rev. A **93**, 012106 (2016).

[47] T. E. Lee, S. Gopalakrishnan, and M. D. Lukin, Unconventional Magnetism via Optical Pumping of Interacting Spin Systems, Phys. Rev. Lett. **110**, 257204 (2013).

[48] E. G. D. Torre, S. Diehl, M. D. Lukin, S. Sachdev, and P. Strack, Keldysh approach for nonequilibrium phase transitions in quantum optics: Beyond the Dicke model in optical cavities, Phys. Rev. A **87**, 023831 (2013).

[49] M. F. Maghrebi and A. V. Gorshkov, Nonequilibrium many-body steady states via Keldysh formalism, Phys. Rev. B **93**, 014307 (2016).

[50] See Appendix A for the full expression of the expansion coefficients.

[51] P. M. Chaikin and T. C. Lubensky, *Principles of Condensed Matter Physics* (Cambridge University Press, Cambridge, 1995).

[52] We would like to stress that this situation is different from other cases of multicritical behavior in dissipative systems, i.e., where already the equilibrium model has a tricritical point [71] or where there is no transition at all in the equilibrium model [28].

[53] H. Kleinert and V. Schulte-Frohlinde, *Critical Properties of Φ^4: Theories* (World Scientific, Singapore, 2001).

[54] See Appendix B for a detailed derivation.

[55] R. Kenna, Finite size scaling for $O(N)\varphi^4$-theory at the upper critical dimension, Nucl. Phys. B **691**, 292 (2004).

[56] See Appendix C for a one-loop calculation based on the perturbative renormalization group.

[57] M. Foss-Feig, J. T. Young, A. V. Victor, A. V. Gorshkov, and M. F. Maghrebi, A solvable family of driven-dissipative many-body systems, arXiv:1703.04626.

[58] N. Henkel, R. Nath, and T. Pohl, Three-Dimensional Roton Excitations and Supersolid Formation in Rydberg-Excited Bose-Einstein Condensates, Phys. Rev. Lett. **104**, 195302 (2010).

[59] G. Pupillo, A. Micheli, M. Boninsegni, I. Lesanovsky, and P. Zoller, Strongly Correlated Gases of Rydberg-Dressed Atoms: Quantum and Classical Dynamics, Phys. Rev. Lett. **104**, 223002 (2010).

[60] J. Honer, H. Weimer, T. Pfau, and H. P. Büchler, Collective Many-Body Interaction in Rydberg Dressed Atoms, Phys. Rev. Lett. **105**, 160404 (2010).

[61] A. W. Glaetzle, M. Dalmonte, R. Nath, C. Gross, I. Bloch, and P. Zoller, Designing Frustrated Quantum Magnets with Laser-Dressed Rydberg Atoms, Phys. Rev. Lett. **114**, 173002 (2015).

[62] R. M. W. van Bijnen and T. Pohl, Quantum Magnetism and Topological Ordering via Rydberg Dressing near Förster Resonances, Phys. Rev. Lett. **114**, 243002 (2015).

[63] Y.-Y. Jau, A. M. Hankin, T. Keating, I. H. Deutsch, and G. W. Biedermann, Entangling atomic spins with a Rydberg-dressed spin-flip blockade, Nat. Phys. **12**, 71 (2016).

[64] J. Zeiher, R. van Bijnen, P. Schauß, S. Hild, J.-y. Choi, T. Pohl, I. Bloch, and C. Gross, Many-body interferometry of a Rydberg-dressed spin lattice, Nat. Phys. **12**, 1095 (2016).

[65] S. Helmrich, A. Arias, and S. Whitlock, Scaling of a driven atomic gas from the weakly-dressed to the quantum critical regime, arXiv:1605.08609.

[66] I. Lindgren, The Rayleigh-Schrödinger perturbation and the linked-diagram theorem for a multi-configurational model space, J. Phys. B **7**, 2441 (1974).

[67] R. Frésard, C. Hackenberger, and T. Kopp, Magnetic transitions in strong coupling expansions for nearly degenerate states, Ann. Phys. (Berlin, Ger.) **524**, 411 (2012).

[68] D. A. Steck, Rubidium 87 D Line Data, revision 2.1.5, http://steck.us/alkalidata.

[69] K. G. Wilson and J. Kogut, The renormalization group and the ϵ expansion., Phys. Rep. **12**, 75 (1974).

[70] N. Goldenfeld, *Lectures on Phase Transitions and the Renormalization Group* (Addison-Wesley, Reading, MA, 1992).

[71] J. Keeling, M. J. Bhaseem, and B. D. Simons, Fermionic Superradiance in a Transversely Pumped Optical Cavity, Phys. Rev. Lett. **112**, 143002 (2014).